Eur. Phys. J. C (2014) 74:3179
DOI 10.1140/epjc/s10052-014-3179-6
THE EUROPEAN PHYSICAL JOURNAL C

Erratum

Erratum to: Comprehensive Bayesian analysis of rare (semi)leptonic and radiative B decays

Frederik Beaujean[1,a], **Christoph Bobeth**[2,b], **Danny van Dyk**[3,c]

[1] C2PAP, Universe Cluster, Ludwig-Maximilians-Universität München, Garching, Germany
[2] Universe Cluster and Institute for Advanced Study, Technische Universität München, Garching, Germany
[3] Theoretische Elementarteilchenphysik, Universität Siegen, Siegen, Germany

Received: 4 November 2014 / Accepted: 11 November 2014 / Published online: 10 December 2014

Erratum to: Eur Phys J C (2014) 74:2897
DOI 10.1140/epjc/s10052-014-2897-0

When revisiting our fits in order to expand the above work, errors in the implementation of analytical expressions of the observables have been encountered. One of these errors affects the branching ratio of $B \to K\ell^+\ell^-$ at low q^2 in the presence of chirality-flipped operators. Carefully checking our results, we also found that systematic uncertainties of the lattice results of the $B \to K^{(*)}$ form factors had been incorrectly neglected.

After correcting these errors, we replace Tables 2 ("Postdiction" rows only), 3, 6, 4, and 5, as well as Figs. 2, 3, and 4. We also replace selected parts of Sect. 4 that are not given in the tables.

While our main conclusions stay as they are, some details are adjusted. Our revised conclusions are given at the end of this erratum.

4 Result

4.1 Statistical approach

For the "selection" data set, we erroneously included the observables P_i' at high q^2. Hence there are now $N = 20$ experimental inputs, two theory constraints, and dim $\boldsymbol{\nu} = 24$.

4.3 Fit in the SM basis

Eq. (4.7) correctly reads

$$\Delta_9 = C_9 - C_9^{\mathrm{SM}} \simeq -1.7 \pm 0.7. \tag{4.7}$$

Our corrected result for the deviation in the $(C_7 - C_9)$ from the SM expectation is $\simeq 2.5\sigma$, and solution A is favored over solution B with $R_A{:}R_B = 82\,\%{:}18\,\%$. Solution A is described by the 1D marginalized 68 % credibility regions

$$\Delta_7 = 0 \pm 0.02, \quad \Delta_9 = -0.5 \pm 0.3, \quad \Delta_{10} = -0.2 \pm 0.3,$$

and loses the model comparison with the SM(ν-only) model with the corrected Bayes factor of

$$\left.\frac{P(\text{full}|\text{SM})}{P(\text{full} \mid \text{SM}(\nu\text{-only}))}\right|_A = 1{:}48. \tag{4.8}$$

Including the $B \to K^*$ form factors from the lattice, we now find

$$\Delta_7 = 0.0 \pm 0.02, \quad \Delta_9 = -0.5 \pm 0.3, \quad \Delta_{10} = -0.1 \pm 0.3,$$

and

$$\left.\frac{P(\text{full (+FF)}|\text{SM})}{P(\text{full (+FF)}|\text{SM}(\nu\text{-only}))}\right|_A = 1{:}43.$$

For the data set "selection", the credibility regions in Fig. 2 are larger now as the observables P_i' at high q^2 are no longer part of it.

4.4 Fit in the extended SM+SM′ basis

We now find that, of all four solutions, A' and D' dominate over B' and C' in terms of the posterior mass:

$$R_{A'}{:}R_{B'}{:}R_{C'}{:}R_{D'} = 37\,\%{:}14\,\%{:}15\,\%{:}34\,\%.$$

The online version of the original article can be found under doi:10.1140/epjc/s10052-014-2897-0.

[a] e-mail: frederik.beaujean@lmu.de
[b] e-mail: bobeth@ph.tum.de
[c] e-mail: vandyk@physik.uni-siegen.de

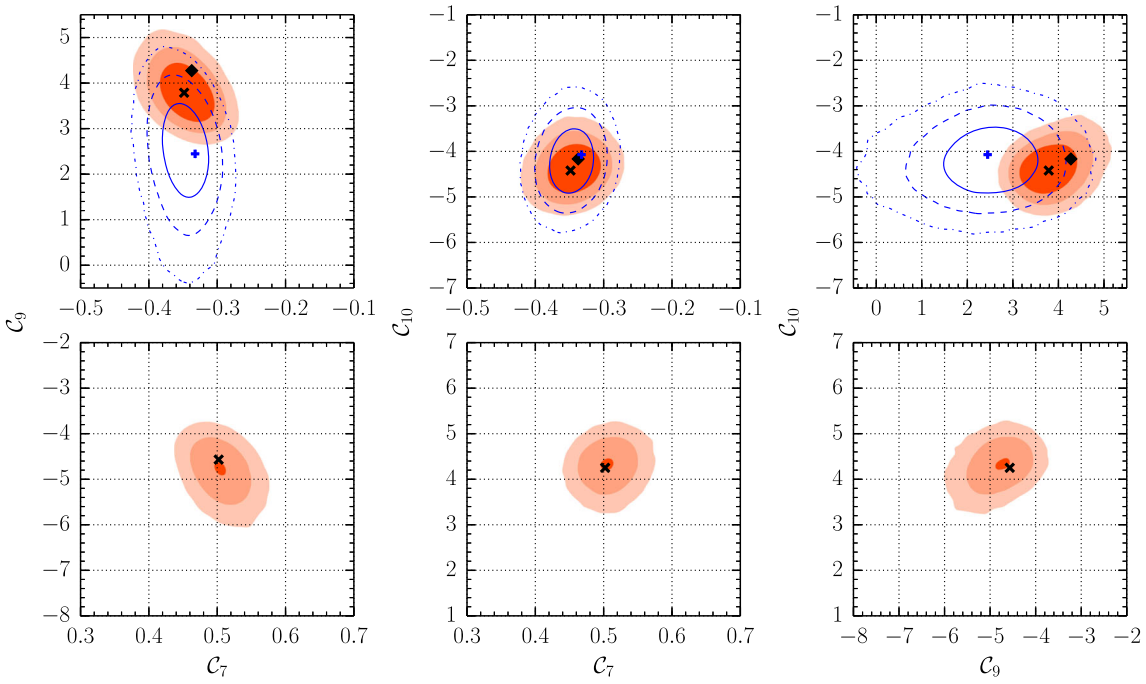

Fig. 2 Credibility regions of the Wilson coefficients $\mathcal{C}_{7,9,10}$ obtained from the fit of the "full" data set after the EPSHEP 2013 conference at 68.3 %, 95.4 %, 99.7 % (*dark*, *normal*, and *light red*) probability. The SM-like solution A (*upper row*) and the flipped-sign solution B (*lower row*) are magnified. Overlaid are the results of the fit to the "selection" data set at 68.3 %, 95.4 %, 99.7 % (*solid*, *dashed*, and *dash-dotted blue lines*) probability. The projection of the SM point is represented by the *black diamond*, whereas the *black* and *blue crosses* mark the best-fit points

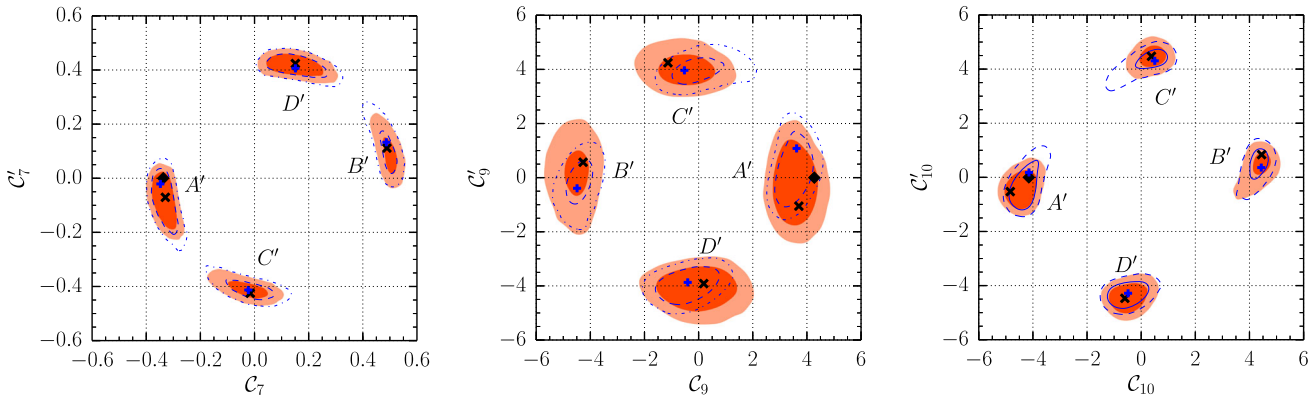

Fig. 3 Credibility regions obtained from the fit in the SM+SM′ model. We show the results of the "full" data set after the EPSHEP 2013 conference at 68.3 % (*dark red*) and 95.4 % (*light red*) probability. The regions from the fit of the "full (+FF)" data set are overlaid by *blue lines* at 68.3 % (*solid*) and 95.4 % (*dashed*) probability. The projection of the SM point is shown by the *black diamond* and the *black* and *blue crosses* mark the best-fit point in the respective 2D plane

The SM-like solution A' exhibits a good fit, with a p value of 0.07. We find agreement between A' and the SM point at $\sim 1\sigma$. The 68 % probability regions are

$$\Delta_7 = 0.01 \pm 0.02, \quad \Delta_9 = -0.8 \pm 0.4, \quad \Delta_{10} = -0.2 \pm 0.3.$$

For further goodness-of-fit criteria for the other solutions we refer to the revised Table 3. The model comparison now yields a Bayes factor of

$$\left.\frac{P(\text{full}|\text{SM+SM}')}{P(\text{full}|\text{SM}(\nu\text{-only}))}\right|_{A'} = 1{:}401. \tag{4.9}$$

For the "full (+FF)" data set, i.e. including lattice results of $B \to K^*$ form factors, we now find

$$\Delta_7 = 0.00^{+0.03}_{-0.02}, \qquad \Delta_9 = -0.8^{+0.4}_{-0.3}, \qquad \Delta_{10} = -0.1 \pm 0.3,$$

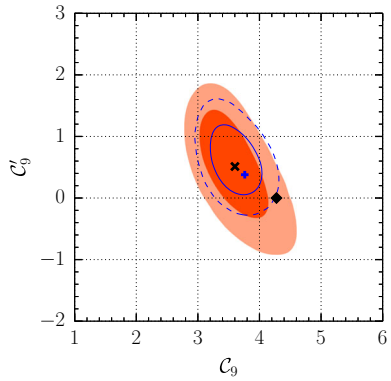

Fig. 4 Credibility regions obtained from the fit in the SM+SM′ (9) model. We show the results of the "full" data set at 68.3 % (*dark red*) and 95.4 % (*red*) probability. The regions from the fit of the "full (+FF)" data set are overlaid by blue lines at 68.3 % (*solid*) and 95.4 % (*dashed*) probability. The projection of the SM point is represented by the *black diamond*, whereas the *black* and *blue crosses* mark the best-fit points

and

$$\left.\frac{P(\text{full (+FF)}|\text{SM+SM}')}{P(\text{full (+FF)}|\text{SM}(\nu\text{-only}))}\right|_{A'} = 1{:}148. \tag{4.10}$$

In the SM+SM′ (9)-scenario, the SM-like solution A' for the fit now reads

$$\Delta_9 = -0.8^{+0.4}_{-0.3}, \qquad \Delta_{9'} = +0.5 \pm 0.6,$$

which remains compatible with the findings of [1]. Our best-fit point is compatible with the SM point at less than 1σ. For solution A', the Bayes factor reads

$$\left.\frac{P(\text{full}|\text{SM+SM}'\ (9))}{P(\text{full}|\text{SM}(\nu\text{-only}))}\right|_{A'} = 1{:}3, \tag{4.11}$$

which is slightly in favor of the SM. However, adding the lattice QCD results on the $B \to K^*$ form factors evens the odds:

Table 3 Goodness of fit and posterior evidence (ratio) for various combinations of constraints and fit models. Individual solutions are labeled as A and B in the SM($\nu-$only) and the SM, and A' through D' in the SM+SM′ and A' in the SM+SM′ (9). The solutions with SM-like and flipped signs of $\mathcal{C}_i$ are $A^{(\prime)}$ and $B^{(\prime)}$, respectively. For the definitions of $P(D|M)$ and R, see Eq. (4.1) in the original article

Scenario	Data set	Solution	χ^2	p value	ln $P(D\|M)$	R
SM(ν-only)	Full	A	109.4	0.12	572.3	1
	Full (+FF)	A	114.5	0.06	580.2	1
	Selection	A	12.4	0.90	118.0	1
SM	Full	A	106.0	0.12	562.1	0.82
		B	110.4	0.07	560.6	0.18
	Full (+FF)	A	109.7	0.08	570.1	0.75
		B	111.8	0.06	569.0	0.25
	Selection	A	6.2	0.99	112.1	1
SM+SM′	Full	A'	107.0	0.07	557.8	0.37
		B'	106.9	0.07	556.8	0.14
		C'	106.2	0.08	556.9	0.15
		D'	105.4	0.09	557.7	0.34
	Full (+FF)	A'	109.7	0.05	566.7	0.35
		B'	106.9	0.07	565.9	0.16
		C'	107.6	0.07	566.0	0.17
		D'	105.5	0.09	566.6	0.32
SM+SM′ (9)	Full	A'	105.7	0.14	568.7	1
	Full (+FF)	A'	110.1	0.08	577.6	1

$$\left.\frac{P(\text{full (+FF)}|\text{SM+SM}'\ (9))}{P(\text{full (+FF)}|\text{SM}(\nu\text{-only}))}\right|_{A'} = 1{:}1. \tag{4.12}$$

5 Conclusions

Our Bayesian analysis indicates that the standard model provides an adequate description of the available measurements of rare leptonic, semileptonic, and radiative B decays. Compared to our previous analysis [5], we determine the Wilson coefficients $\mathcal{C}_{7,9,10}$ more accurately, dominantly due

Table 2 Postdictions for the optimized observables $P'_{4,5,6}$ in various q^2 bins. Note that the uncertainties correspond to 68 % credibility intervals that arise from variation of all fit parameters. Note further that the postdiction of $\langle P'_5\rangle_{[1,6]}$ in SM+SM′ consists of two distinct regions around -0.3 and -0.4 from solutions $(A'+B')$ and $(C'+D')$, respectively. †: Values have been adjusted to match the theory convention for the observable

Source	$\langle P'_4\rangle_{[1,6]}$	$\langle P'_4\rangle_{[14.18,16]}$	$\langle P'_4\rangle_{[16,19]}$	$\langle P'_5\rangle_{[1,6]}$	$\langle P'_5\rangle_{[14.18,16]}$	$\langle P'_5\rangle_{[16,19]}$	$\langle P'_6\rangle_{[1,6]}$	$\langle P'_6\rangle_{[14.18,16]}$	$\langle P'_6\rangle_{[16,19]}$
Postdictions: this work, "full" data set									
SM(ν-only)	$0.56^{+0.05}_{-0.05}$	$+1.12^{+0.03}_{-0.03}$	$1.24^{+0.02}_{-0.03}$	$-0.27^{+0.02}_{-0.03}$	$-0.84^{+0.04}_{-0.05}$	$-0.66^{+0.04}_{-0.04}$	$-0.054^{+0.005}_{-0.005}$	$\mathcal{O}(10^{-4})$	$\mathcal{O}(10^{-4})$
SM	$0.58^{+0.06}_{-0.05}$	$+1.12^{+0.03}_{-0.03}$	$1.23^{+0.03}_{-0.02}$	$-0.28^{+0.03}_{-0.03}$	$-0.86^{+0.04}_{-0.04}$	$-0.67^{+0.04}_{-0.04}$	$-0.054^{+0.005}_{-0.006}$	$\mathcal{O}(10^{-4})$	$\mathcal{O}(10^{-4})$
SM+SM′	$0.54^{+0.07}_{-0.06}$	$+1.19^{+0.02}_{-0.03}$	$1.28^{+0.01}_{-0.02}$	$-0.39^{+0.10}_{-0.04}$	$-0.76^{+0.04}_{-0.04}$	$-0.58^{+0.03}_{-0.03}$	$-0.054^{+0.006}_{-0.006}$	$\mathcal{O}(10^{-4})$	$\mathcal{O}(10^{-4})$

Table 4 The 68- and 95 %-credibility intervals and the local modes of the marginalized 1D posterior distributions of the Wilson coefficients at $\mu = 4.2$ GeV, $P(\mathcal{C}_i|D)$, $i = 7, 9, 10, 7', 9', 10'$, for nominal priors of nuisance parameters in the various scenarios. Note that for the SM+SM′-scenario the individual solutions cannot be disentangled within the 1D posterior distributions, unlike for the SM-scenario. For comparison, the SM values of the Wilson coefficients read $\mathcal{C}_7^{\rm SM} = -0.34, \mathcal{C}_9^{\rm SM} = +4.27, \mathcal{C}_{10}^{\rm SM} = -4.17, \mathcal{C}_{7'}^{\rm SM} = -0.01, \mathcal{C}_{9'}^{\rm SM} = \mathcal{C}_{10'}^{\rm SM} = 0$

Scenario		SM "selection"	SM "full"		SM+SM′ "full"
Solution		*A*	*A*	*B*	
$\mathcal{C}_7$	68 %	$[-0.37, -0.33]$	$[-0.37, -0.31]$	–	$[-0.38, -0.30] \cup [+0.06, +0.19] \cup [+0.47, +0.51]$
	95 %	$[-0.39, -0.31]$	$[-0.39, -0.30]$	$[+0.47, +0.53]$	$[-0.38, -0.28] \cup [-0.12, +0.26] \cup [+0.44, +0.54]$
	Mode	-0.35	-0.34	$+0.50$	$-0.33 \wedge +0.12 \wedge +0.50$
$\mathcal{C}_9$	68 %	$[+1.85, +3.20]$	$[+3.25, +4.21]$	–	$[-1.18, +0.75] \cup [+2.95, +4.01]$
	95 %	$[+1.06, +3.85]$	$[+3.03, +4.56]$	$[-5.30, -4.30]$	$[-5.32, -3.91] \cup [-1.89, +1.46] \cup [+2.69, +4.36]$
	Mode	$+2.53$	$+3.75$	-4.67	$-4.48 \wedge +0.01 \wedge +3.52$
$\mathcal{C}_{10}$	68 %	$[-4.66, -3.74]$	$[-4.80, -4.00]$	–	$[-4.79, -4.05] \cup [-0.90, +0.50]$
	95 %	$[-5.12, -3.28]$	$[-5.05, -3.71]$	$[+3.88, +4.72]$	$[-5.04, -3.80] \cup [-1.23, +0.92] \cup [+3.73, +4.81]$
	Mode	-4.19	-4.36	$+4.32$	$-4.42 \wedge -0.53 \wedge +4.44$
$\mathcal{C}_{7'}$	68 %	–	–	–	$[-0.43, -0.39] \cup [-0.14, -0.01] \cup [+0.38, +0.44]$
	95 %	–	–	–	$[-0.46, -0.36] \cup [-0.19, +0.17] \cup [+0.36, +0.46]$
	Mode	–	–	–	$-0.41 \wedge -0.07 \wedge +0.41$
$\mathcal{C}_{9'}$	68 %	–	–	–	$[-4.60, -3.55] \cup [-1.10, +0.74] \cup [+3.72, +4.07]$
	95 %	–	–	–	$[-5.04, -3.29] \cup [-1.97, +1.62] \cup [+3.28, +4.68]$
	Mode	–	–	–	$-4.03 \wedge -0.09 \wedge +3.85$
$\mathcal{C}_{10'}$	68 %	–	–	–	$[-4.78, -4.11] \cup [-0.92, +0.34] \cup [+4.28, +4.45]$
	95 %	–	–	–	$[-5.03, -3.86] \cup [-1.17, +0.92] \cup [+3.86, +4.87]$
	Mode	–	–	–	$-4.40 \wedge -0.46 \wedge +4.40$

to the reduction of the experimental uncertainties in the exclusive decays and the addition of the inclusive decay $B \to X_s\gamma$.

Contrary to all similar analyses, our fits include the theory uncertainties explicitly through nuisance parameters. We observe that tensions in the angular and optimized observables in $B \to K^*\ell^+\ell^-$ decays can be lifted through (10–20) % shifts in the transversity amplitudes at large recoil due to subleading contributions. These shifts are present within the SM as well as the model-independent extension of real-valued Wilson coefficients $\mathcal{C}_{7,9,10}$. For the scenarios introducing additional chirality-flipped coefficients $\mathcal{C}_{7',9',10'}$, the shifts reduce to a few percent (except $\zeta^{L\perp}_{K^*}$). We find $|\mathcal{C}_{9',10'}| \lesssim 5$ at 95 % probability; see Fig. 3 and Table 4, for the right-handed couplings, which holds in the absence of scalar and tensor contributions. These constraints are insensitive to the shape (Gaussian vs. flat) of the priors of subleading corrections.

Among the information inferred from the data are constraints on the parameters of the $B \to K^{(*)}$ form factors. We have performed all fits with and without the very recent lattice $B \to K^*$ form factor predictions [4]. In both cases, the posterior ranges of the Wilson coefficients $\mathcal{C}_{7,7',10,10'}$ are essentially the same apart from minor shifts in $\mathcal{C}_{9,9'}$. Again in both cases, the posteriors of the $B \to K^*$ form-factor parameters are very similar. This comes as a surprise given the large difference in prior uncertainties but implies that the combination of measurements supports the lattice input, even independently of the scenario.

The rough picture emerging from the current data may be summarized as follows. The low-q^2 $B \to K^*\ell^+\ell^-$ data prefer a negative new-physics contribution to $\mathcal{C}_9$ [6], which is not supported by $B \to K\ell^+\ell^-$ data unless one allows a positive contribution to $\mathcal{C}_{9'}$ (or alternatively $\mathcal{C}_{10'}$) [1]. Our Bayesian analysis shows strong support for the standard model SM(ν-only) compared to additional new physics in Wilson coefficients $\mathcal{C}_{7,9,10}$ in the SM-scenario and/or chirality-flipped $\mathcal{C}_{7',9',10'}$ in the SM+SM′-scenario in terms of Bayes factors. Only a reduced scenario SM+SM′ (9) of the two Wilson coefficients $\mathcal{C}_{9,9'}$ comes close to the standard model. Including the $B \to K^*$ form-factor lattice predictions, the model comparison suggests that scenario SM+SM′ (9) can provide an explanation of the data as efficient as in the standard model with a Bayes factor of 1:1.

A substantial reduction of uncertainties can be expected for LHCb, CMS, and ATLAS measurements of $B^0 \to K^{*0}\ell^+\ell^-$ and $B^+ \to K^+\ell^+\ell^-$ once they publish the analysis of their 2012 data sets. It should also be mentioned that $B \to K^*\gamma$ and $B \to K^{(*)}\ell^+\ell^-$ results from Belle are not based on the final reprocessed data set and that BaBar's angu-

Table 5 Compilation of the pull values in units of σ at the SM-like best-fit points A in the SM fit (left columns) and A' in the SM+SM$'$ fit (right columns), listed per experiment and observable. Only pull values for fits with the "full" data set are listed. The single CLEO measurement of $\mathcal{B}(B \to K^*\gamma)$ has a pull value $+0.3\sigma$ in both the SM and the SM+SM$'$ fits. The pull values for the SM(ν-only) fit deviate by less than 0.3σ from those of the SM fit for the "full" data set, with the exception of $+2.3\sigma$ for the LHCb measurement of $\langle P_5' \rangle_{[1,6]}$. The pull values in scenario SM+SM$'$ with the "full (+FF)" data set deviate by less than 0.4σ from those given for SM+SM$'$ "full", except for the LHCb measurements of $\langle A_T^{(2)} \rangle_{[1,6]}$ with $+1.1\sigma$, $\langle A_T^{(\mathrm{re})} \rangle_{[1,6]}$ with $+0.6\sigma$ and $\langle P_5' \rangle_{[1,6]}$ with $+1.2\sigma$. The pull values for SM "full (+FF)" deviate by less than 0.3σ from those of SM "full" except for $\langle P_5' \rangle_{[1,6]}$ with slightly increased by $+0.4\sigma$

Observable		SM full, solution A						SM+SM$'$ full, solution A'					
		ATLAS	BaBar	Belle	CDF	CMS	LHCb	ATLAS	BaBar	Belle	CDF	CMS	LHCb
$B \to X_s\gamma$	$\mathcal{B}$	–	−0.1	+0.4	–	–	–	–	+0.2	+0.8	–	–	–
$B \to X_s\ell^+\ell^-$	$\langle \mathcal{B} \rangle_{[1,6]}$	–	+0.5	+0.3	–	–	–	–	+0.2	−0.2	–	–	–
$B_s \to \mu^+\mu^-$	$\mathcal{B}$	–	–	–	–	−0.7	−0.7	–	–	–	–	−0.4	−0.4
	$\mathcal{B}$	–	+0.7	−1.2	–	–	–	–	+0.5	−1.4	–	–	–
$B \to K^*\gamma$	$S + C$	–	+0.4	+0.7	–	–	–	–	+0.8	+0.4	–	–	–
	$\langle \mathcal{B} \rangle_{[1,6]}$	–	+0.3	+0.3	+0.3	–	−0.8	–	+0.2	+0.3	+0.2	–	−0.9
	$\langle \mathcal{B} \rangle_{[14.18,16]}$	–	+1.1	+0.3	+0.9	–	+0.8	–	+1.0	+0.2	+0.8	–	+0.6
$B \to K\ell^+\ell^-$	$\langle \mathcal{B} \rangle_{[16,18]}$	–	–	–	–	–	+0.7	–	–	–	–	–	+0.6
	$\langle \mathcal{B} \rangle_{[16,23]}$	–	+0.0	+1.5	−1.8	–	–	–	−0.1	+1.4	−1.9	–	–
	$\langle \mathcal{B} \rangle_{[18,22]}$	–	–	–	–	–	−0.8	–	–	–	–	–	−1.0
	$\langle \mathcal{B} \rangle_{[1,6]}$	–	+0.5	−0.7	+0.3	+0.9	−0.4	–	+0.5	−0.7	+0.3	+0.8	−0.5
	$\langle \mathcal{B} \rangle_{[14.18,16]}$	–	+1.0	−0.2	+1.1	−1.3	−0.6	–	+1.1	−0.1	+1.2	−1.1	−0.4
	$\langle \mathcal{B} \rangle_{[16,19]}$	–	−0.6	**+2.6**	−1.4	+0.9	−0.2	–	−0.5	**+2.7**	−1.3	+1.0	−0.1
	$\langle A_{\mathrm{FB}} \rangle_{[1,6]}$	−0.9	−1.9	−1.2	−1.9	−0.4	–	−0.7	−1.6	−1.1	−1.7	−0.1	–
	$\langle A_{\mathrm{FB}} \rangle_{[14.18,16]}$	−0.3	+0.8	−1.1	−0.6	+1.3	−1.6	−0.4	+0.7	−1.2	−0.7	+1.2	−1.9
	$\langle A_{\mathrm{FB}} \rangle_{[16,19]}$	**+2.1**	+0.2	−1.7	−0.2	−0.5	+1.0	+1.9	+0.1	−1.8	−0.3	−0.8	+0.8
	$\langle F_L \rangle_{[1,6]}$	**−2.5**	**−3.4**	+0.4	+1.2	+1.1	+1.1	**−2.5**	**−3.3**	+0.4	+1.3	+1.1	+1.1
	$\langle F_L \rangle_{[14.18,16]}$	−0.5	+0.4	−1.8	+0.7	+1.3	−0.4	−0.4	+0.5	−1.8	+0.8	+1.5	−0.2
	$\langle F_L \rangle_{[16,19]}$	+0.1	+1.2	−1.5	−1.5	+1.3	+0.5	+0.2	+1.3	−1.4	−1.5	+1.4	+0.6
	$\langle A_T^{(2)} \rangle_{[1,6]}$	–	–	–	−0.2	–	+0.6	–	–	–	−0.3	–	−0.5
	$\langle A_T^{(2)} \rangle_{[14.18,16]}$	–	–	–	+0.5	–	+1.1	–	–	–	+0.6	–	+1.3
$B \to K^*\ell^+\ell^-$	$\langle A_T^{(2)} \rangle_{[16,19]}$	–	–	–	−0.1	–	−0.5	–	–	–	−0.1	–	−0.4
	$\langle A_T^{(\mathrm{re})} \rangle_{[1,6]}$	–	–	–	–	–	+1.2	–	–	–	–	–	+1.7
	$\langle P_4' \rangle_{[1,6]}$	–	–	–	–	–	−0.1	–	–	–	–	–	+0.0
	$\langle P_4' \rangle_{[14.18,16]}$	–	–	–	–	–	**−2.4**	–	–	–	–	–	**−2.4**
	$\langle P_4' \rangle_{[16,19]}$	–	–	–	–	–	−1.2	–	–	–	–	–	−1.2
	$\langle P_5' \rangle_{[1,6]}$	–	–	–	–	–	+1.4	–	–	–	–	–	+1.7
	$\langle P_5' \rangle_{[14.18,16]}$	–	–	–	–	–	+0.0	–	–	–	–	–	−0.2
	$\langle P_5' \rangle_{[16,19]}$	–	–	–	–	–	+0.2	–	–	–	–	–	−0.1
	$\langle P_6' \rangle_{[1,6]}$	–	–	–	–	–	+1.1	–	–	–	–	–	+1.0
	$\langle P_6' \rangle_{[14.18,16]}$	–	–	–	–	–	+0.7	–	–	–	–	–	+0.7
	$\langle P_6' \rangle_{[16,19]}$	–	–	–	–	–	−0.8	–	–	–	–	–	−0.8

lar analysis of $B \to K^*\ell^+\ell^-$ is still preliminary. It remains to be seen whether these improved analyses further substantiate the present hints of a 1 to 2σ deviation from the SM prediction in $\mathcal{C}_9$.

In our opinion, however, there remain two major challenges on the theory side. The first is to improve our analytic knowledge of the $1/m_b$ corrections to the exclusive decay amplitudes. The second is to reduce the uncertainty from hadronic form factors, especially at low q^2. Without improvements on either, there is little prospect to distinguish between small NP effects and large subleading corrections. Another point of concern are potentially large duality-violating effects that render the OPE at high q^2 invalid. They have been estimated, though model-dependently, to be small [7]. In this

Table 6 1D-marginalized posterior results at 68 % probability in comparison to the prior inputs for the various $B \to K^*$ (upper rows) and $B \to K$ (middle two rows) form-factor parameters. The results are shown for the "full" (left) and "full (+FF)" (right) data set in various scenarios. The priors for the "full" data set comprise LCSR [2] inputs combined with the additional constraints Eqs. (6.1)–(6.3); see the original article, and $B \to K$ lattice results [3], whereas for "full (+FF)" the $B \to K^*$ lattice results [4] are added. Note that the marginalization has been performed over all solutions A, B in the case of SM and $A' - D'$ in the case of SM+SM′

	No $B \to K^*$ lattice				$B \to K^*$ lattice			
	Prior	SM(ν-only)	SM	SM+SM′	Prior	SM(ν-only)	SM	SM+SM′
$V(0)$	$0.35^{+0.14}_{-0.09}$	$0.40^{+0.03}_{-0.03}$	$0.40^{+0.03}_{-0.03}$	$0.39^{+0.03}_{-0.03}$	$0.36^{+0.03}_{-0.03}$	$0.38^{+0.03}_{-0.02}$	$0.38^{+0.03}_{-0.02}$	$0.37^{+0.02}_{-0.02}$
b_1^V	$-4.8^{+0.7}_{-0.5}$	$-4.7^{+0.7}_{-0.5}$	$-4.8^{+0.5}_{-0.4}$	$-4.9^{+0.5}_{-0.3}$	$-4.8^{+0.7}_{-0.4}$	$-4.6^{+0.8}_{-0.4}$	$-4.8^{+0.7}_{-0.4}$	$-4.9^{+0.6}_{-0.3}$
$A_1(0)$	$0.28^{+0.08}_{-0.07}$	$0.24^{+0.03}_{-0.02}$	$0.25^{+0.03}_{-0.02}$	$0.26^{+0.03}_{-0.03}$	$0.28^{+0.04}_{-0.03}$	$0.26^{+0.03}_{-0.02}$	$0.26^{+0.03}_{-0.02}$	$0.27^{+0.03}_{-0.03}$
$b_1^{A_1}$	$0.4^{+0.7}_{-1.0}$	$0.4^{+0.6}_{-0.6}$	$0.5^{+0.6}_{-0.6}$	$0.5^{+0.6}_{-0.7}$	$0.5^{+0.5}_{-0.7}$	$0.3^{+0.5}_{-0.6}$	$0.4^{+0.5}_{-0.6}$	$0.2^{+0.6}_{-0.5}$
$A_2(0)$	$0.24^{+0.13}_{-0.07}$	$0.23^{+0.04}_{-0.04}$	$0.24^{+0.04}_{-0.04}$	$0.24^{+0.05}_{-0.04}$	$0.28^{+0.05}_{-0.05}$	$0.25^{+0.04}_{-0.03}$	$0.26^{+0.04}_{-0.04}$	$0.27^{+0.04}_{-0.04}$
$b_1^{A_2}$	$-0.5^{+2.1}_{-1.7}$	$-0.6^{+1.5}_{-1.3}$	$-0.9^{+1.6}_{-1.1}$	$-0.8^{+1.4}_{-1.2}$	$-1.4^{+1.3}_{-0.9}$	$-1.4^{+1.0}_{-0.9}$	$-1.5^{+1.1}_{-0.7}$	$-1.4^{+1.2}_{-0.8}$
$f_+(0)$	$0.33^{+0.04}_{-0.03}$	$0.30^{+0.02}_{-0.02}$	$0.30^{+0.02}_{-0.02}$	$0.29^{+0.02}_{-0.02}$	$0.33^{+0.04}_{-0.03}$	$0.30^{+0.02}_{-0.02}$	$0.31^{+0.02}_{-0.02}$	$0.29^{+0.02}_{-0.02}$
$b_1^{f_+}$	$-2.3^{+0.6}_{-0.8}$	$-3.1^{+0.5}_{-0.5}$	$-3.1^{+0.5}_{-0.5}$	$-3.2^{+0.4}_{-0.5}$	$-2.3^{+0.6}_{-0.8}$	$-3.1^{+0.5}_{-0.5}$	$-2.9^{+0.4}_{-0.6}$	$-3.4^{+0.6}_{-0.5}$
$V(0)/A_1(0)$	$1.3^{+0.3}_{-0.3}$	$1.6^{+0.2}_{-0.1}$	$1.6^{+0.2}_{-0.2}$	$1.5^{+0.2}_{-0.2}$	$1.2^{+0.2}_{-0.1}$	$1.5^{+0.2}_{-0.1}$	$1.4^{+0.2}_{-0.2}$	$1.4^{+0.2}_{-0.2}$
$A_2(0)/A_1(0)$	$0.99^{+0.10}_{-0.15}$	$0.95^{+0.08}_{-0.08}$	$0.96^{+0.07}_{-0.08}$	$0.96^{+0.08}_{-0.08}$	$0.98^{+0.09}_{-0.10}$	$0.98^{+0.07}_{-0.07}$	$0.99^{+0.07}_{-0.08}$	$0.98^{+0.07}_{-0.07}$

regard, the experimental verification of certain relations [8] among angular observables in $B \to K^* \ell^+ \ell^-$ that are predicted by the OPE would be very desirable. In the case that some of these relations are not fulfilled, the analysis of the breaking pattern can provide information on duality violation but also on additional new-physics scalar and tensor interactions.

References

1. W. Altmannshofer, D.M. Straub, Eur. Phys. J. C **73**, 2646 (2013). doi:10.1140/epjc/s10052-013-2646-9
2. A. Khodjamirian, T. Mannel, A. Pivovarov, Y.M. Wang, JHEP **1009**, 089 (2010). doi:10.1007/JHEP09(2010)089
3. C. Bouchard, G.P. Lepage, C. Monahan, H. Na, J. Shigemitsu, Phys. Rev. D **88**, 054509 (2013). doi:10.1103/PhysRevD.88.054509
4. R.R. Horgan, Z. Liu, S. Meinel, M. Wingate, Phys. Rev. D **89**, 094501 (2014). doi:10.1103/PhysRevD.89.094501
5. F. Beaujean, C. Bobeth, D. van Dyk, C. Wacker, JHEP **1208**, 030 (2012). doi:10.1007/JHEP08(2012)030
6. S. Descotes-Genon, J. Matias, J. Virto, Phys. Rev. D **88**, 074002 (2013). doi:10.1103/PhysRevD.88.074002
7. M. Beylich, G. Buchalla, T. Feldmann, Eur. Phys. J. C **71**, 1635 (2011). doi:10.1140/epjc/s10052-011-1635-0
8. C. Bobeth, G. Hiller, D. van Dyk, Phys. Rev. D **87**, 034016 (2013). doi:10.1103/PhysRevD.87.034016